Fermilab

Fermilab-Conf-09-172-APC April 2009

BEAM LOSSES AND BACKGROUND LOADS ON COLLIDER DETECTORS DUE TO BEAM-GAS INTERACTIONS IN THE LHC*†

A.I. Drozhdin, N.V. Mokhov, S.I. Striganov

FNAL, Batavia, IL 60510, U.S.A.

Abstract

With a fully-operational high-efficient collimation system in the LHC, nuclear interactions of circulating protons with residual gas in the machine beam pipe can be a major source of beam losses in the vicinity of the collider detectors, responsible for the machine-induced backgrounds. Realistic modeling of Coulomb scattering, elastic and inelastic interactions of 7-TeV protons with nuclei in the vacuum chamber of the cold and warm sections of the LHC ring - with an appropriate pressure profile - is performed with the STRUCT and MARS15 codes. Multi-turn tracking of the primary beams, propagation of secondaries through the lattice, their interception by the tertiary collimators TCT as well as properties of corresponding particle distributions at the CMS and ATLAS detectors are studied in great detail and results presented in this paper.

*Work supported by Fermi Research Alliance, LLC under contract No. DE-AC02-07CH11359 with the U.S. Department of Energy.

†Presented paper at Particle Accelerator Conference (PAC09), May 4-8, 2009, Vancouver, Canada.

BEAM LOSSES AND BACKGROUND LOADS ON COLLIDER DETECTORS DUE TO BEAM-GAS INTERACTIONS IN THE LHC*

A.I. Drozhdin, N.V. Mokhov#, S.I. Striganov, FNAL, Batavia, IL 60510, U.S.A.

Abstract

With a fully-operational high-efficient collimation system in the LHC, nuclear interactions of circulating protons with residual gas in the machine beam pipe can be a major source of beam losses in the vicinity of the collider detectors, responsible for the machine-induced backgrounds. Realistic modeling of Coulomb scattering, elastic and inelastic interactions of 7-TeV protons with nuclei in the vacuum chamber of the cold and warm sections of the LHC ring - with an appropriate pressure profile - is performed with the STRUCT and MARS15 codes. Multi-turn tracking of the primary beams, propagation of secondaries through the lattice, their interception by the tertiary collimators TCT as well as properties of corresponding particle distributions at the CMS and ATLAS detectors are studied in great detail and results presented in this paper.

MACHINE-INDUCED BACKGROUNDS

Beam loss in the vicinity of interaction points (IP) at the LHC is an outstanding source of background rates in the collider detectors, called machine-induced backgrounds (MIB) [1, 2]. As shown in [3], the relative importance of this component can be comparable to that from the pp-collisions at early operation of the LHC because MIB is mostly related to beam intensity and not luminosity, and tuning the machine will require substantial time and efforts.

In this paper we consider the design LHC beam with 2808 bunches of 7-TeV protons in the scrubbed machine. At nominal operation, there are three sources of MIB for the experiments [2]:

- **Collimator tails**: protons escaping the betatron and momentum cleaning insertions (IP7 and IP3, respectively) and being intercepted by the tertiary collimators TCT. This term, related to the inefficiency of the main collimation system, is called “tails from collimators” or “tertiary beam halo”. The TCTs are situated between the neutral beam absorber (TAN) and D2 separation dipole at about 148m on each side of IP1 and IP5. They are set to 8.3σ to fully protect the triplet magnets. For the betatron cleaning in IP7 at the rate of 8.3×10^9 p/s, a 10-hr beam lifetime and nominal intensity, the loss rates on the TCTs are 2.61×10^6 p/s and 4.28×10^6 p/s for Beam-2 approaching IP5 and Beam-1 approaching IP1, respectively [2].
- **Inelastic beam-gas**: nuclear inelastic (including quasi-elastic and diffractive) interactions of the incoming beam with the residual gas. Products of such interactions in straight sections and arcs upstream of the experiments have a good chance to be lost on limiting apertures in front of the collider detectors. The rate of beam-gas interactions is proportional to the beam intensity and residual gas pressure in the beam pipe. Detailed studies since the first papers on MIB in LHC [1, 3] have shown that relatively large-angle inelastic nuclear interactions in the 550-m regions upstream of IP1 and IP5 are mostly responsible for the beam-gas component of MIB. The total number of inelastic and quasi-elastic nuclear interactions in these regions for each of the beams coming to IP1 and IP5 is 3.07×10^6 p/s [2].
- **Elastic beam-gas**: nuclear elastic – coherent and incoherent (quasi-elastic) - interactions as well as Coulomb scattering on residual gas around the ring.

First two sources are studied in great detail in thorough MARS15 [4] calculations. Modeling approach and results of calculations of energy-dependent particle fluxes in the machine components, tunnel, and ATLAS and CMS experimental halls as described in [2]. Third component is described in this paper.

ELASTIC BEAM-GAS INTERACTIONS

As described in [5, 6], the main process of beam-gas interaction, Coulomb scattering, results in slow diffusion of protons from the beam core causing emittance growth. These particles increase their betatron amplitudes gradually during many turns and are intercepted by the main collimators before they reach other limiting apertures. Similar behavior takes place for small-angle elastic nuclear scattering. For certain beam parameters, large-angle nuclear elastic and Coulomb scattering can behave quite differently [6]. Such processes can result in a substantial increase of the betatron amplitude and, if not intercepted by the main collimators, the scattered protons can be lost in the vicinity of the experimental insertions, predominantly giving rise to the “scraping” rate on the TCTs and adding to MIB in the detectors.

A differential cross section of nuclear elastic scattering can be parameterized as a sum of two exponential distributions. The slope of coherent elastic scattering has weak energy dependence and can be taken from [7]. The slope of quasi-elastic scattering is close to the slope of pp elastic scattering at high energies. An approximation [8] of experimental data on the slope of elastic pp-scattering at 2-2000 GeV/c is extrapolated to 7 TeV. Total cross

*Work supported by Fermi Research Alliance, LLC, under contract No. DE-AC02-07CH11359 with the U.S. Department of Energy.
#mokhov@fnal.gov

sections of these processes are calculated using the Glauber model with inelastic corrections. The contribution of electromagnetic elastic (Coulomb) scattering is calculated using the screened Rutherford cross section. Atomic and nuclear screening is taken into account.

The calculated differential cross sections of proton-carbon elastic scattering at 7 TeV are shown in Fig. 1. At angles $\theta > 7$ μrad, responsible for beam loss in LHC, the role of Coulomb scattering is diminishing.

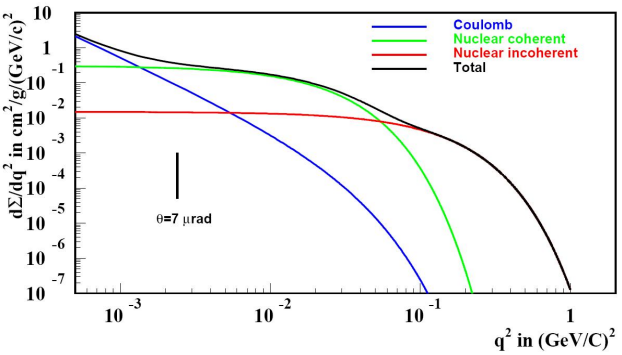

Figure 1: Differential cross sections of proton-carbon elastic scattering at 7 TeV.

MODELING BEAM-GAS INTERACTIONS

As with beam-gas inelastic collisions, the rate of Coulomb scattering and nuclear elastic beam-gas interactions is proportional to the beam intensity and residual gas pressure in the beam pipe. Longitudinally it follows the pressure maps [9]. The points of beam interactions with residual gas nuclei are sampled from the data shown in Fig. 2.

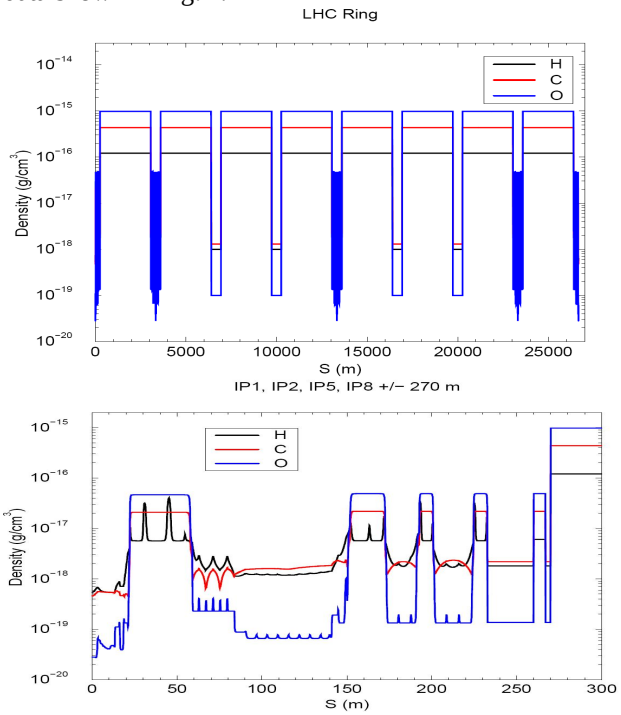

Figure 2: Density of residual gas molecules in the LHC ring (top) and interaction regions (bottom).

For the nominal beam current of 0.6 A, one gets 1.154×10^8 nuclear elastic and Coulomb interactions per second in the ring for each of the two beams. Multi-turn modeling of these interactions was performed separately for Beam 1 and Beam 2 with the STUCT code [10]. All the apertures were included in the model. Fig. 2 shows calculated beam loss distribution around the ring for Beam2. The first maximum at ~6500 m corresponds to IP7, second at ~13182 m to tertiary collimators at IP5, third at ~20000 m to IP3, and fourth to the tertiary collimators at IP1.

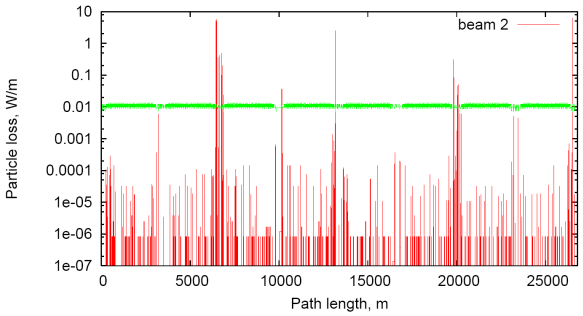

Figure 3: Beam loss distribution along the LHC ring for Beam 2 elastically interacted with residual gas.

The Beam 2 loss rates (MHz) are 35.78 (IP7), 3.07 (TCT.R5), 7.19 (TCT.L1) and 2.08 (rest of the ring). Similarly, the loss rates (MHz) for Beam 1 are 33.81 (IP7), 7.05 (TCT.L5), 4.68 (TCT.R1) and 2.58 (rest of the ring). With the mandatory tertiary collimators in IP1 and IP5, the products of elastic beam-gas interactions in the ring are locally intercepted by these TCTs. With the arcs being the main source of this component, the role of the limiting aperture of the betatron cleaning system in IP7 is quite obvious: for Beam 1, ¼ and ¾ of the ring contribute to loss rate in IP1 and IP5, correspondingly, while for Beam 2, the situation for IP1 and IP5 is reversed.

Fig. 4 shows a distribution of the number of turns an elastically scattered proton of Beam 1 or Beam 2 makes before being intercepted by the IP1 and IP5 tertiary collimators. Most of the scattered protons are intercepted by TCTs on the first turn, while some of them make 2, 3 and more turns before being lost on the tertiary collimators.

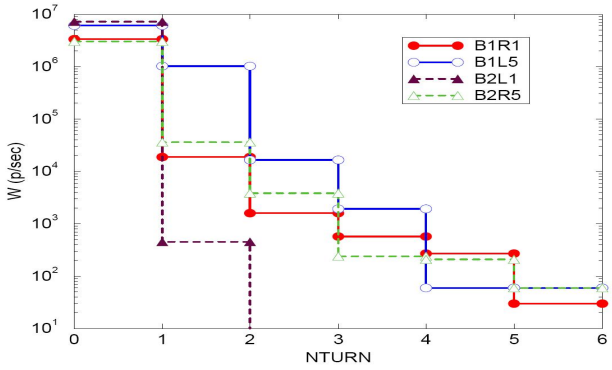

Figure 4: Contribution of elastically scattered protons to the loss rates on TCTs as a function of a number of turns.

The contributions to the proton loss rate on the tertiary collimators from the incoherent (quasi-elastic), coherent and Coulomb scattering processes in the ring are 46, 52.6 and 1.4 percent, respectively, not very different for Beam 1 and 2 as well as for IP1 and IP5. Tagging the gas components involved in these processes, reveals that H, C and O contribute 17, 29 and 54 percent, respectively, to the losses on TCTs, again quite similar for both beams and both high-luminosity insertions.

LOADS ON ATLAS AND CMS

The full MARS15 shower simulations are performed in IP1 and IP5 with the source terms on their TCTs generated for Beam 1 and 2 as described in the previous section. As with two other sources – "collimator tails" and "inelastic beam-gas" – all the details of geometry, materials and magnetic fields around IP are included in the model at 22.6 < z < 150 m and r < 12 m. For the simulated nominal conditions of Beam 2, the sources in IP5 (R) are rather similar (rate-wise): 2.61 MHz on TCT.B2R5 for "collimator tails", 3.07 MHz at 22.6 < z < 550 m for "inelastic beam-gas", and 3.07 MHz on TCT.B2R5 for "elastic beam-gas". Distributions of all particle types are calculated and analyzed at the machine-detector interface plane z=22.6 m as in [2]. As an example, Fig. 5 shows the lateral distributions of particle fluxes at the IP5 (R) interface plane.

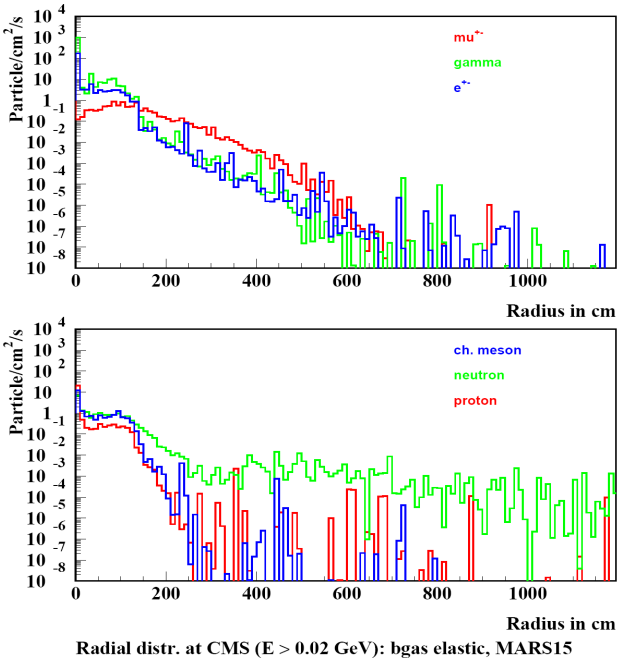

Figure 5: Radial distributions of particle fluxes (E>20 MeV) at z=22.6 m from IP5 (R) for "elastic beam-gas".

Not a surprise that with the same loss rates on TCT (a "point-like" source at z~148 m with respect to the interface plane), the distributions for "elastic beam-gas" are very similar to those for "collimator tails". At the same time, radial distributions of particle fluxes at the interface plane for the "inelastic beam-gas" case are very different [2]. The dominant component is now muons from decays of pions and kaons generated in large-angle beam-gas interactions distributed along a few hundred meters. The highest interaction rate happens in the arcs at z > 270 m from IP (Fig. 2), with average pion trajectories tangent to the ring. Therefore, muons and other particles, which accompany muons, arrive at the IP1 and IP5 interface planes at large distances from the beam axis, resulting in pretty flat lateral distributions in the orbit plane in the direction outside the ring center (Fig. 6). The loads to sub-detectors at radii r < 2 m are not so different for both inelastic and elastic beam-gas sources.

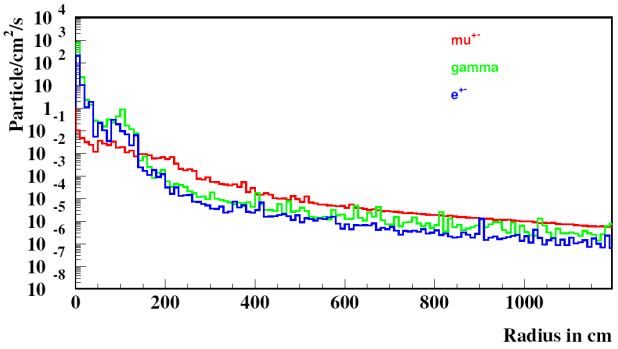

Figure 6: Radial distributions of particle fluxes (E>20 MeV) at z=22.6 m from IP for "inelastic beam-gas" [2].

REFERENCES

[1] N.V. Mokhov, Nucl. Physics B, 51A (1996) 210.

[2] N.V. Mokhov, T. Weiler, "Machine-Induced Backgrounds: Their Origin and Loads on ATLAS/CMS", Fermilab-Conf-08-147-APC (2008).

[3] A.I. Drozhdin, M. Huhtinen, N.V. Mokhov, Nucl. Instr. And Meth. A381 (1996) 531.

[4] N.V. Mokhov, "The Mars Code System User's Guide", Fermilab-FN-628 (1995); N.V. Mokhov, S.I. Striganov, "MARS15 Overview", in *Proc. of Hadronic Shower Simulation Workshop*, Fermilab, September 2006, AIP Conf. Proc. 896, p. 50 (2007); Fermilab-Conf-07/008-AD (2007); http://www-ap.fnal.gov/MARS/

[5] N.V. Mokhov, V.I. Balbekov, "Beam and Luminosity Lifetime", in *Handbook of Accelerator Physics and Engineering*, *2nd Printing*, Ed. A.W. Chao, M. Tigner, P. 218, World Scientific (2002).

[6] A.I. Drozhdin, V.A. Lebedev, N.V. Mokhov et al., "Beam Loss and Backgrounds in the CDF and D0 Detectors due to Nuclear Elastic Beam-Gas Scattering"', PAC'03, Portland, Oregon, 2003; also Fermilab-FN-734 (2003). http://www.JACoW.org.

[7] A. Schiz et al., Phys. Rev., D21 (1980) 3010.

[8] J.P. Burq et al Nucl. Phys. B217, (1983) 285.

[9] A. Rossi, CERN-LHC-Project-Report 783 (2004).

[10] I.S. Baishev, A.I. Drozhdin, N.V. Mokhov, X. Yang, "STRUCT Program User's Reference Manual", http://www-ap.fnal.gov/users/drozhdin/.